Hippocampal Morphometry Study by Automated Surface Fluid Registration and Its Application to Alzheimer's Disease

Jie Shi[1], Yuting Wang[2], Paul M. Thompson[3], Yalin Wang[1]

[1]School of Computing, Informatics and Decision Systems Engineering, ASU, Tempe, AZ 85281, USA
[2]Mathematics Department, UCLA, Los Angeles, CA 90095, USA
[3]Lab. of Neuro Imaging, UCLA School of Medicine, Los Angeles, CA 90095, USA
jie.shi@asu.edu

Abstract. Alzheimer's disease (AD) is a severe and growing public health crisis. Efforts are underway to look for AD early detection in an efficient manner. Among all the AD biomarkers, hippocampal atrophy assessed on high-resolution T1-weighted MRI is the best established and validated. Hippocampal morphometry is increasingly used in the AD research, with modeling the hippocampus as a 3D parametric surface mesh. However, a major question in the analysis is how to align corresponding surface regions across subjects. Here we develop a system for detecting AD symptoms on hippocampal surfaces with an automated surface fluid registration method, which is based on conformal surface representation and mutual information regularized image fluid registration. Since conformal mappings are diffeomorphic and the mutual information method is able to drive a diffeomorphic flow that is adjusted to enforce appropriate surface correspondences in the surface parameter domain, combining conformal and fluid mappings will generate 3D shape correspondences that are diffeomorphic. We also incorporate in the system a novel method to compute curvatures using surface conformal parameterization. Experimental results in three hippocampal datasets show that the new system outperformed an early similar method and the popular SPHARM tool.

1 Introduction

Alzheimer's disease (AD) doubles in frequency of onset every 5 years after age 60, afflicting 1% of those aged 60 to 64, and 30-40% of those over 85. Many MRI-based measures of atrophy in several structural measures, including whole-brain, hippocampus [14, 16, 19], and ventricular enlargement [19], etc., correlate closely with changes in cognitive performance, supporting their validity as markers of AD progression [8]. Among all the biomarkers, hippocampal atrophy assessed on high-resolution T1-weighted MRI is the best established and validated. As a result, detection of valid and efficient morphometry changes in hippocampus and their correlation with other cognitive functions and biomarkers becomes a

key research topic for clinical diagnosis and monitoring of patients with suspected Alzheimer's disease. Although most hippocampus analysis used volume as the atrophy measurement [10], recent researches [1, 16, 19, 26] demonstrated that surface-based subcortical structure analysis may offer more advantages because these methods studied patterns of hippocampal subfield atrophy and produced detailed point-wise correlation between atrophy and cognitive functions/biological markers [19].

Brain surface deformation studies typically require the computation of dense correspondence vector fields that match one surface with another. Many brain surface registration methods have been proposed [6, 20, 27].Often, higher order correspondences must be enforced between specific anatomical points and curved landmarks lying within the two surfaces. This can be achieved by first mapping each of the 3D surfaces to canonical parameter spaces such as a sphere [7] or a planar domain [21]. A flow, computed in the parameter space of the two surfaces [4], induces a correspondence field in 3D. Artificial neural networks can rule out or favor certain types of feature matches [15]. Correspondences may be determined by using a minimum description length (MDL) principle, based on the compactness of the covariance of the resulting shape model [5]. A key direction in surface registration research has been the computation of a diffeomorphic surface map that also matches automatically identified surface features.

Using holomorphic 1-forms, a global conformal parameterization can be developed to conformally map a surface with complex topology (e.g., a surface with branching topology) to a set of rectangular domains in the Euclidean plane. The resulting parameterization helps in discretizing partial differential equations (PDEs) for smoothing, denoising, or matching signals defined on the surface. The mutual information (MI) method has been widely used to drive a diffeomorphic flow in image registration. By adjusting the mutual information method to enforce appropriate surface correspondences in the parameter domain, any scalar-valued signals defined on the surfaces can also be aligned using the same flow field. Conformal maps and fluid registration techniques can be combined to avoid having to define a large set of manually-defined landmarks to constrain brain surface correspondences. Since they generate diffeomorphic mappings, conformal and fluid mappings together could generate 3D shape correspondences that are diffeomorphic (i.e., smooth one-to-one correspondences). In [21, 22], Wang et al. proposed an automated surface fluid registration method based on conformal mapping and mutual information regularized image fluid registration and applied it to register human faces and hippocampus. Here we develop a system based on this technique for studying hippocampus in AD and incorporate a novel method to compute surface curvatures as proposed in [12]. Our major contributions can be summarized as: (1). Introduction of a new stable method to compute surface curvatures. (2). An automated hippocampal surface registration system validated in three AD datasets with better performance than a previous similar method [23] and SPHARM [18]. (3). The system will be publicly available [24]. Last, although the current system finds applications in AD detection, it is a general method which may be applied to many other applications.

2 Method

2.1 Surface Conformal Parameterization

Let S be a surface in $\mathbb{R}^3$ with an atlas $\{(U_\alpha, z_\alpha)\}$, where (U_α, z_α) is a coordinate chart defined on S. The atlas thus is a set of consistent charts with smooth transition functions between overlapping charts. Here $z_\alpha : U_\alpha \to \mathbb{C}$ maps an open set $U_\alpha \subset S$ to a complex plane $\mathbb{C}$. If on any chart (U_α, z_α) in the atlas, the Riemannian metric or the first fundamental form can be formulated as $ds^2 = \lambda(z_\alpha)^2 dz_\alpha d\bar{z_\alpha}$, and the transition maps $z_\beta \circ z_\alpha^{-1} : z_\alpha(U_\alpha \bigcap U_\beta) \to z_\beta(U_\alpha \bigcap U_\beta)$ are holomorphic, the atlas could be called conformal. Given a conformal atlas, a chart is compatible with the atlas if adding this chart still generates a conformal atlas. A conformal structure is obtained by adding all possible compatible charts to a conformal atlas. A Riemann surface is a surface with a conformal structure. One coordinate chart in the conformal structure introduces a *conformal parameterization* between a surface patch and the image plane. The conformal parameterization is angle-preserving and intrinsic to the surface geometry.

Let (x_α, y_α) be the local parameter on the chart (U_α, z_α) on S, a differential 1-form in (x_α, y_α) can be defined as

$$\omega = f(x_\alpha, y_\alpha)dx_\alpha + g(x_\alpha, y_\alpha)dy_\alpha \tag{1}$$

where f, g are smooth functions. ω is a closed 1-form, if in each local parameter (x_α, y_α), $\frac{\partial f}{\partial y_\alpha} - \frac{\partial g}{\partial x_\alpha} = 0$. If ω is the gradient of another function defined on S, it can be called an exact 1-form. An exact 1-form is also a closed 1-form. If a closed 1-form ω satisfies $\frac{\partial f}{\partial x_\alpha} + \frac{\partial g}{\partial y_\alpha} = 0$, then it is a harmonic 1-form. The gradient of a harmonic 1-form is an exact harmonic 1-form. The Hodge star operator acting on a differential 1-form gives the conjugate differential 1-form

$$^*\omega = -g(x_\alpha, y_\alpha)dx_\alpha + f(x_\alpha, y_\alpha)dy_\alpha \tag{2}$$

Intuitively, the conjugate 1-form $^*\omega$ is obtained by rotating ω by a right angle everywhere. If ω is harmonic, so is its conjugate $^*\omega$. The holomorphic 1-form consists of a pair of conjugate harmonic 1-forms:

$$\tau = \omega + \sqrt{-1}^*\omega \tag{3}$$

For a Riemann surface S with genus $g > 0$, its conformal structure can always be represented in terms of a holomorphic 1-form basis, which is a set of $2g$ functions $\tau_i : K_i \to R^2, i = 1, 2 \cdots, 2g$ [22]. Any holomorphic 1-form τ is a linear combination of these functions. This finite-dimensional linear space generates all possible conformal parameterizations of surface S and the quality of a global conformal parameterization is fundamentally determined by the choice of the holomorphic 1-form [22]. Then the conformal parameterization ϕ at point p can be computed by integrating the holomorphic 1-form: $\phi(p) = \int_\gamma \tau$, where γ is any path joining p to a fixed point c on the surface. Figure 1 (a) illustrates a brain cortical surface and its conformal parameterization to a square.

2.2 Surface Conformal Representation

It has been known that surface registration requires defining a lot of landmarks in order to align corresponding functional regions. Labeling features could be accurate but time-consuming. Here we show that surface conformal parameterization could represent surface geometric features, thus avoiding the manual definition of landmarks.

For a general surface and its conformal parameterization $\phi : S \to \mathbb{R}^2$, the conformal factor at a point p can be determined by the formulation:

$$\lambda(p) = \frac{\text{Area}(B_\epsilon(p))}{\text{Area}(\phi(B_\epsilon(p)))} \tag{4}$$

where $B_\epsilon(p)$ is an open ball around p with a radius ϵ. The conformal factor λ encodes a lot of geometric information about the surface and can be used to compute curvatures and geodesic. In our system, we compute the surface mean curvatures only from the derivatives of the conformal parameterization as proposed in [12], instead of the three coordinate functions and the normal, which are generally more sensitive to digitization errors. Mathematically, the mean curvature is defined as:

$$H = \frac{1}{2\lambda}\text{sign}(\phi)|\Delta\phi|, \text{ where } \text{sign}(\phi) = \frac{< \Delta\phi, \overrightarrow{N} >}{|\Delta\phi|}. \tag{5}$$

Using this formulation of H, we need to use the surface normal $\overrightarrow{N}$ only when computing $\text{sign}(\phi)$, which takes the value 1 or -1. Thus, the surface normal does not need to be accurately estimated and still we can get more accurate mean curvatures. Using the Gauss and Codazzi equations, one can prove that the conformal factor and mean curvature uniquely determine a closed surface in $\mathbb{R}^3$, up to a rigid motion. We call them the *conformal representation* of the surface. Figure 1 (b) shows the computed conformal factor (left) and mean curvature (right) on a hippocampal surface with color indices according to the values. Since conformal factor and mean curvature could represent important surface features and they are intrinsic to the surface, they may be used for surface registration.

2.3 Surface Fluid Registration Regularized by Mutual Information

After computing intrinsic geometric features, we align surfaces in the parameter domain with a fluid registration technique.Using conformal mapping, we essentially convert the surface registration problem to an image registration problem. The mutual information (MI) method has been successfully used to drive a diffeomorphic flow in rigid [25] and non-rigid [13, 17] image registration. Image registration will be optimized when MI between two images is maximized. For MI to work, a monotonic mapping in grayscales between images is not required, so images from different modalities can be registered [11]. Hermosillo et al. [9] adopted linear elasticity theory to regularize the variational maximization of MI.

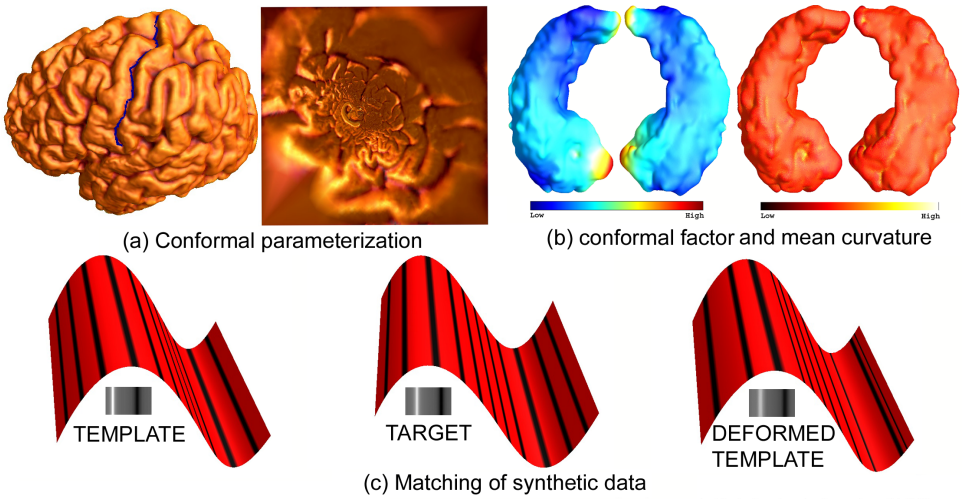

Fig. 1. Illustration of conformal parameterization (a) and geometric features (b). (c) shows the matching of geometric features in the 2D parameter domains using fluid registration with synthetic surfaces. Geometric features on 3D surfaces were computed and mapped to 2D conformal parameter domains.

D'Agostino et al. [3] extended this approach to a viscous fluid scheme allowing large local deformations, while maintaining smooth, one-to-one topology [2]. We call this approach MI regularized fluid registration.

In [21, 22], Wang et al. proposed an automated surface fluid registration method combining conformal mapping and image fluid registration [3]. Let I_1, I_2 be the conformal representations of the target and the deforming template surfaces, respectively, the MI between two surfaces was defined as [21, 22]

$$I(u) = \int_{\mathbb{R}^2} p_u(i_1, i_2) log \frac{p_u(i_1, i_2)}{p(i_1)p_u(i_2)} di_1 di_2 \tag{6}$$

where $p(i_1) = P(I_1(x) = i_1), p_u(i_2) = P(I_2(x-u) = i_2)$, and $p_u(i_1, i_2) = P(I_1(x) = i_1 \ \& \ I_2(x-u) = i_2)$. Since conformal mapping and MI regularized fluid registration generate diffeomorphic mappings, a diffeomorphic surface-to-surface mapping is then recovered that matches surfaces in 3D. In our system, we adopt their methods of conformal mapping and fluid registration. However, our system differs from theirs in the computation of surface features as introduced in Sec. 2.2. The new way to compute mean curvature is more stable and less sensitive to normal computation, thus gives better representation of the surface features for registration.

3 Results

3.1 Synthetic Surface Registration Result

First, we illustrate the algorithm on synthetic surfaces. Figure 1 (c) illustrates a synthetic surface example. A pair of simple S-shape surfaces were generated. Corresponding 2D images were generated based on the sum of the local conformal factor and the mean curvature, expressed in the conformal parameterization domain. Some black horizontal lines were drawn on the surfaces to show equal distances on the surfaces and represent the differences in their shapes.The locations of the highest and lowest intensities are different (as shown by the positions of the horizontal stripes in the 2D images below). Using surface-based fluid registration, in the last image, the obtained horizontal line positions demonstrated an improved matching between features lying in the two surfaces.

In this experiment, we aim to visually explain the work flow of the algorithm. First, we conformally mapped each surface onto a planar domain and computed their conformal representation by combining conformal factor and mean curvature. Second, we scaled the conformal representation to form the 2D feature images as shown by the first two 2D images in Fig. 1 (c). As we pointed out in Sec. 2.2, the 2D images, i.e. the conformal representations of the surfaces clearly show the characteristics of the surfaces. Third, by registering the two feature images using fluid registration method, we induced a change in both the template feature image and the template surface. The last image in Fig. 1 (c) demonstrates that without changing the shape of the surface, the features on the template surface are well aligned with the target surface.

3.2 Hippocampal Surface Morphometry in Alzheimer's Disease

In this experiment, we test the robustness of our system by applying it to two clinical studies of hippocampal changes in Alzheimer's disease (AD). In our system, we leave two holes at the front and back of the hippocampal surface, representing its anterior junction with the amygdala, and its posterior limit as it turns into the white matter of the fornix. The resulting structure can then be logically represented as an open boundary genus-one surface, i.e., a cylinder. To better visualize the matching of surface features, we chose to encode surface features using a compound scalar function based on the local conformal factor and the mean curvature. A similar technique for AD study in hippocampus was proposed in [23], but with surface registration using constrained harmonic map. We take their method as a comparison. After the cross-subject registration is computed with one target surface selected, we examine shape differences using the multivariate tensor-based morphometry (MTBM) [23]. MTBM computes statistics from the Riemannian metric tensors that retain the full information in the deformation tensor fields, thus is more powerful in detecting surface differences than many other statistics [23].

Figure 2 illustrates the experimental results on a group of hippocampal surface models extracted from 3D brain MRI scans of 12 individuals with AD and

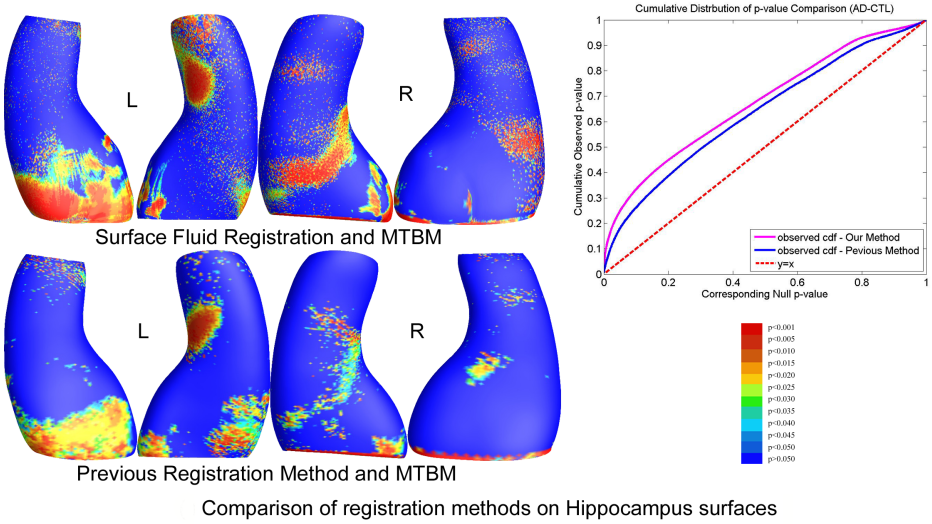

Fig. 2. The comparison of our method and a previous similar method on map of local shape differences (p-values), based on the multivariate TBM method with hippocampal surfaces in 12 AD versus 14 control subjects [19].

14 matched healthy control subjects, the same dataset as in [19], where the data was manually traced by experienced neurologists. With MTBM, we can see that the significant areas detected with two methods are consistent.But with surface fluid registration, we detected larger areas with more significant group differences in the surface parameterization tensor, which is related to the relative area of regions in disease versus normality.The overall statistical significance of these group difference maps, based on permutation testing of the suprathreshold area of statistics (and therefore corrected for multiple comparisons) were p=0.0063 for the left hippocampal surface and 0.0298 for the right. This outperformed the previous method [23] (0.0205 for the left hippocampal surface and 0.1026 for the right). The cumulative distribution function (CDF) plot shows the comparison of resulting p-values for each method. While the line $y = x$ represents null hypothesis, which is according to no difference, steeper curve shows more differences detected.

Figure 3 illustrates the experimental results on another hippocampal dataset from the Alzheimer's Disease Neuroimaging Initiative (ADNI) dataset (http://www.loni.ucla.edu/ADNI). Mild cognitive impairment (MCI) is an intermediate stage between the expected cognitive decline of normal aging and the more pronounced decline of dementia. If MCI could be found and treated, the risk of AD will be significantly reduced. However, at MCI stage, changes in brain surface are not significant thus impose more difficulty on the detection. Here we randomly chose 40 AD, 40 MCI, and 40 control subjects to test the effectiveness of our system. The hippocampus data was automatically segmented by a prior work [14]. With MTBM, we can see that, in the three experiments, our system

demonstrated better results than the previous method. Particularly, our system gave better MCI detection results when comparing with both AD and control subjects. In the experiment, all group difference p-maps were corrected using false discovery rate (FDR). The FDR method decides whether a threshold can be assigned to the statistical map that keeps the expected FDR below 5% (i.e., no more than 5% of the voxels are false positive findings). The CDF plots show the uncorrected p-values (as in a conventional FDR analysis). The x value at which the CDF plot intersects the $y = 20x$ line represents the FDR corrected p-value or q-value. It is the highest statistical threshold that can be applied to the data, for which at most 5% false positives are expected in the map. In general, a larger q-value indicates a more significant difference in the sense that there is a broader range of statistic threshold that can be used to limit the rate of false positives to at most 5%. The use of the $y = 20x$ line is related to the fact that significance is declared when the volume of suprathreshold statistics is more than 20 times that expected under the null hypothesis. Table 1 gives the FDR corrected p-values comparison.

3.3 Comparison with SPHARM

In this study, we tested our system on the whole ADNI baseline dataset (http://www.loni.ucla.edu/ADNI). The dataset consists of 233 healthy controls, 410 subjects with MCI, and 200 patients with AD. We excluded 1 subject from the control group and 2 subjects from the MCI group due to name duplication. For subjects with duplicated names, we retained the one which is the repeated scan. The hippocampal surfaces were automatically segmented using FIRST (http://www.fmrib.ox.ac.uk/fsl/first/index.html). FIRST is an integrated surface analysis tool developed as part of the FSL library, which is written mainly by members of the Analysis Group, FMRIB, Oxford, UK. We compared our system's results with the popular SPHARM tool [18] in surface registration on the same dataset. We adopted the suggested parameters for hippocampus in the manual of SPHARM [18]. In this experiment, 1 subject from each group (AD, MCI, control) failed the FIRST segmentation step probably due to the original images' resolution or contrast. After FIRST segmentation, we extracted the left and right hippocampi and saved each of them into a binary image. We fed the binary images as the input of both systems. As a result, 231 control, 199 AD, and 407 MCI subjects were successfully registered by our system, which shows the robustness of the system compared with SPHARM, in which 5 control, 17 AD, 14 MCI subjects failed either due to segmentation failure or parameterization failure. Fig. 4 shows the experimental results. From the p-map and the CDF plots, we can see that, with MTBM, our system outperformed the SPHARM

	Our Method	Prior Method [23]
AD-CTL	0.0476	0.0467
MCI-AD	0.0217	0.0199
MCI-CTL	0.0221	0.0185

Table 1. FDR corrected p-values on hippocampal surfaces

in all three group difference studies. Table 2 gives the FDR corrected p-values comparison. Considering fairness, we also made comparisons by excluding those subjects that failed in SPHARM from our system in the statistical study. Table 3 gives the FDR corrected p-values comparison with the failed subjects excluded, i.e., 226 control, 182 AD, and 393 MCI subjects were studied in this experiment. From the table, we can see that our system still outperformed SPHARM on this dataset. Furthermore, because AD and MCI failed more than control subjects, the AD-MCI group has been more affected as expected.

4 Conclusion and Future Work

We develop an automated surface fluid registration system for hippocampal surface registration. Experiments on different types of AD hippocampal datasets all demonstrate our system's stronger statistical power. Ongoing work is to apply this system to automatically map lateral ventricle enlargements in Alzheimer's disease and those at risk.

References

1. Apostolova, L.G., et al.: Subregional hippocampal atrophy predicts Alzheimer's dementia in the cognitively normal. Neurobiol Aging 31(7), 1077–1088 (2008)
2. Christensen, G.E., et al.: Deformable templates using large deformation kinematics. IEEE Trans Image Process 5(10), 1435–1447 (1996)
3. D'Agostino, E., et al.: A viscous fluid model for multimodal non-rigid image registration using mutual information. Med Image Anal 7(4), 565–575 (2003)
4. Davatzikos, C.: Spatial normalization of 3D brain images using deformable models. J. Comp. Assisted Tomography 20(4), 656–665 (1996)
5. Davies, R.H., et al.: A minimum description length approach to statistical shape modeling. IEEE Trans Med Imaging 21(5), 525–537 (2002)
6. Durrleman, S., et al.: Sparse approximation of currents for statistics on curves and surfaces. In: Med. Image Comp. Comput.-Assist. Intervention, Proceedings. vol. 11, pp. 390–398 (2008)
7. Fischl, B., et al.: High-resolution inter-subject averaging and a coordinate system for the cortical surface. Human Brain Mapping 8(4), 272–284 (1999)
8. Frisoni, G.B., et al.: The clinical use of structural MRI in Alzheimer disease. Nature Reviews Neurology 6(2), 67–77 (2010)
9. Hermosillo, G.: Ph.D. thesis, Université de Nice (INRIAROBOTVIS), Sophia Antipolis, France (2002)
10. Holland, D., et al.: Subregional neuroanatomical change as a biomarker for Alzheimer's disease. In: Proc. Natl. Acad. Sci. USA (2009)
11. Kim, B., et al.: Mutual information for automated unwarping of rat brain autoradiographs. Neuroimage 5(1), 31–40 (1997)

	Our Method	SPHARM [18]
AD-CTL	0.0485	0.0459
MCI-AD	0.0215	0.0047
MCI-CTL	0.0483	0.0288

Table 2. FDR corrected p-values on hippocampal surfaces.

12. Lui, L.M., et al.: Computation of curvatures using conformal parameterization. Communications in Information and Systems 8(1), 1–16 (2008)
13. Meyer, C.R., et al.: Demonstration of accuracy and clinical versatility of mutual information for automatic multimodality image fusion using affine and thin-plate spline warped geometric deformations. Medical Image Analysis 1(3), 195–206 (1997)
14. Morra, J.H., et al.: Automated mapping of hippocampal atrophy in 1-year repeat MRI data from 490 subjects with Alzheimer's disease, mild cognitive impairment, and elderly controls. Neuroimage 45(1 Suppl), S3–15 (2009)
15. Pitiot, A., et al.: Learning object correspondences with the observed transport shape measure. In: Proceedings of Information Processing in Medical Imaging (IPMI 2003). pp. 25–37 (2003)
16. Qiu, A., et al.: Regional shape abnormalities in mild cognitive impairment and Alzheimer's disease. Neuroimage 45(3), 656–661 (2009)
17. Rueckert, D., et al.: Nonrigid registration using free-form deformations: application to breast MR images. IEEE Trans Med Imaging 18(8), 712–721 (1999)
18. Styner, M., et al: Framework for the statistical shape analysis of brain structures using SPHARM-PDM. The Insight Journal pp. 242–250 (2006)
19. Thompson, P.M., et al.: Mapping hippocampal and ventricular change in Alzheimer disease. Neuroimage 22(4), 1754–1766 (2004)
20. Vaillant, M., et al.: Surface matching via currents. In: Proceedings of Information Processing in Medical Imaging (IPMI 2005). vol. 19, pp. 381–392 (2005)
21. Wang, Y., et al.: Automated surface matching using mutual information applied to Riemann surface structures. In: Med. Image Comp. Comput.-Assist. Intervention, Proceedings, Part II. pp. 666–674 (2005)
22. Wang, Y., et al.: Mutual information-based 3D surface matching with applications to face recognition and brain mapping. In: Proc. Intl Conf. Computer Vision. pp. 527–534 (2005)
23. Wang, Y., et al.: Multivariate tensor-based brain anatomical surface morphometry via holomorphic one-forms. In: Med. Image Comp. Comput.-Assist. Intervention, Proceedings. vol. 12, pp. 337–344 (2009)
24. Wang, Y.: Multivariate tensor-based subcortical morphometry system (2011), http://gsl.lab.asu.edu/conformal.htm
25. West, J., et al.: Comparison and evaluation of retrospective intermodality brain image registration techniques. J. Comp. Assisted Tomography 21(4), 554–566 (1997)
26. Yushkevich, P.A.: Continuous medial representation of brain structures using the biharmonic PDE. Neuroimage 45(1 Suppl), S99–110 (2009)
27. Zhong, J., et al.: Multi-manifold diffeomorphic metric mapping for aligning cortical hemispheric surfaces. Neuroimage 49(1), 355–365 (2010)

	Our Method	SPHARM [18]
AD-CTL	0.0486	0.0459
MCI-AD	0.0195	0.0047
MCI-CTL	0.0483	0.0288

Table 3. FDR corrected p-values on hippocampal surfaces (with failed subjects excluded).

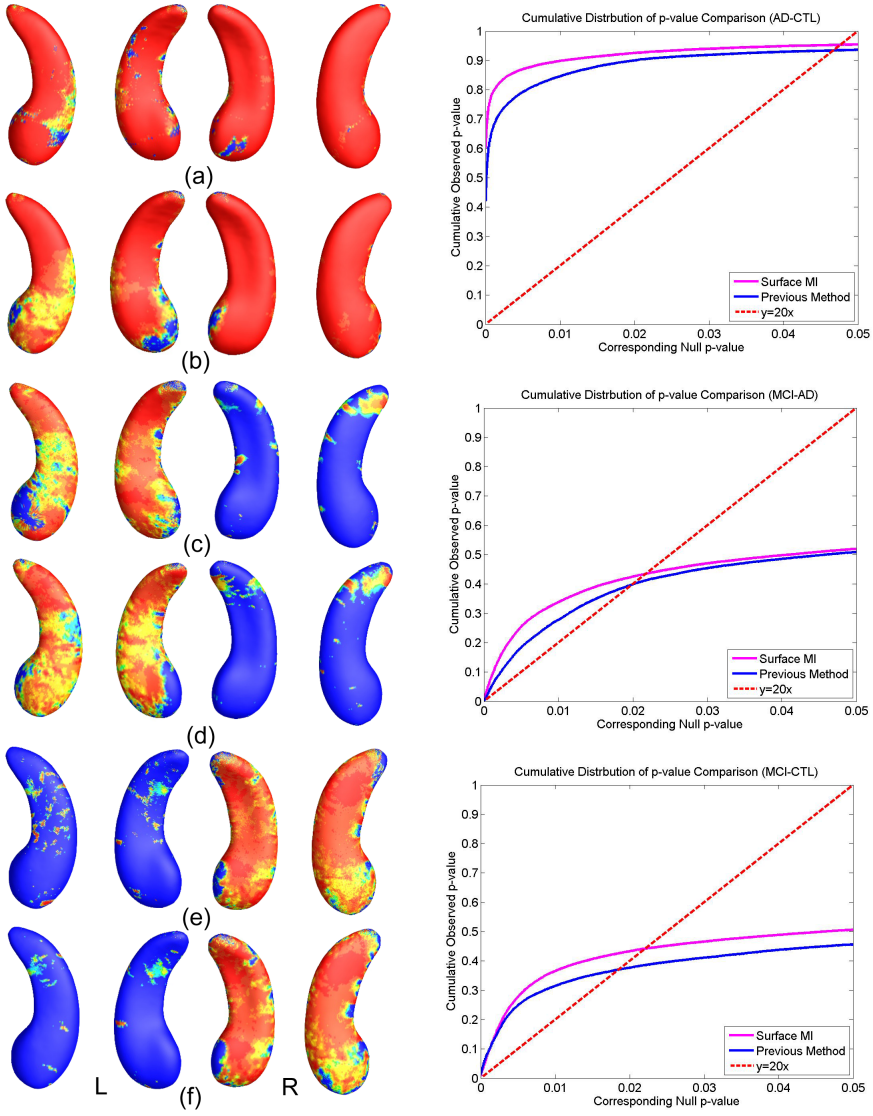

Fig. 3. Comparison of surface fluid registration and the previous method on map of local shape differences (p-values), based on the mutivariate TBM method with hippocampal surfaces in 40 AD, 40 MCI, and 40 control subjects which were automatically segmented [14]. (a), (c), (e) are our results on group difference between AD and control, MCI and AD, MCI and control, respectively. Similarly, (b), (d), (f) are results of a prior work [23] on AD and control, MCI and AD, MCI and control, respectively. The p-map color scale is the same as Figure 2.

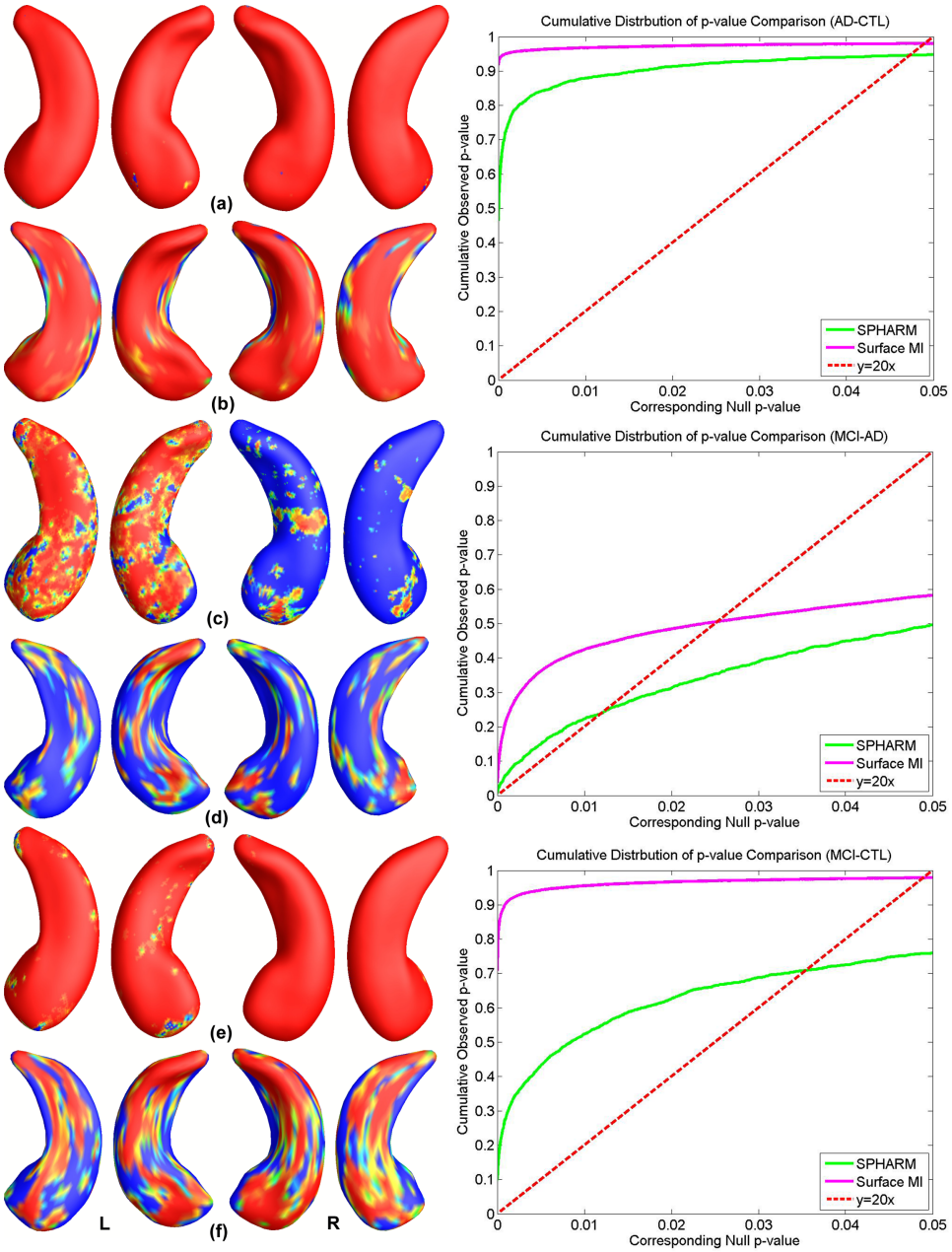

Fig. 4. Comparison of surface fluid registration and SPHARM on map of local shape differences (p-values), based on the mutivariate TBM method with hippocampal surfaces from ADNI baseline data, which were automatically segmented by FIRST. (a), (c), (e) are our results on group difference between AD and control, MCI and AD, MCI and control, respectively, in 231 control, 199 AD, and 407 MCI subjects. Similarly, (b), (d), (f) are results of SPHARM on AD and control, MCI and AD, MCI and control, respectively, in 226 control, 182 AD, and 393 MCI subjects. The p-map color scale is the same as Figure 2.